SMALL STRAIN STIFFNESS AND DAMPING RATIO OF PISA CLAY FROM SURFACE WAVE TESTS

Foti, S. (2003). *Géotechnique* **53**, No. 5, 455–461

Small-strain stiffness and damping ratio of Pisa clay from surface wave tests

S. FOTI*

Small-strain stiffness and damping ratio are important parameters for modelling the dynamic behaviour of soils. In particular, the experimental evaluation of the damping ratio is problematic, especially for hard-to-sample soils. Surface wave tests have proven to be a reliable tool for the in-situ determination of soil stiffness at very small strains. Recently, the simultaneous determination of stiffness and damping ratio has been developed. The technique is based on the measurement and inversion of dispersion and attenuation curves of Rayleigh waves. In this paper a novel transfer function procedure is presented. The application to data collected at the Leaning Tower of Pisa testing site, where many results from previous in-situ and laboratory test are available for comparison, is reported.

KEYWORDS: dynamics; in-situ testing; site investigation; stiffness; waves and wave loading

La rigidité et le facteur d'amortissement des petites déformations sont des paramètres importants pour la modélisation du comportement dynamique des sols. Notamment, les évaluations expérimentales du facteur d'amortissement posent problème, surtout pour les sols difficiles à échantillonner. Les essais d'onde de surface se sont révélés être des outils fiables pour déterminer in situ la rigidité des sols à faibles déformations. Récemment, une détermination simultanée de la rigidité et du facteur d'amortissement a été développée. La technique est basée sur le mesurage et l'inversion des courbes de dispersion et d'atténuation des ondes de Raleigh. Dans cet exposé, nous présentons une nouvelle méthode de fonction de transfert. Nous appliquons cette méthode aux données collectées sur le site d'essai de la Tour de Pise, où un grand nombre de résultats obtenus lors de tests antérieurs in situ et en laboratoire sont disponibles pour permettre les comparaisons.

INTRODUCTION

Seismic tests are widely used in geotechnical engineering to identify the small-strain mechanical parameters of soils. Indeed, the propagation of seismic waves is associated with very small strains, and the propagation can be interpreted in the framework of linear elastic laws, using simple relationships to link the velocity of propagation of waves to the elastic parameters of the medium.

One critical aspect is the quantification of the dissipative behaviour. Experimental tests have shown that, even at very small strains, soils exhibit energy dissipation during cyclic loading, but the corresponding deformations are still completely reversible (Ishihara, 1996). A linear viscoelastic framework can be used to interpret and model this behaviour (Ishihara, 1996). In geotechnical engineering energy dissipation is typically quantified in terms of the damping ratio, D, the ratio between energy dissipated and total energy during a complete hysteresis cycle (Kramer, 1996). Alternative but equivalent definitions are used in other disciplines, for example the quality factor $Q = 1/(2D)$ in seismology (Aki & Richards, 1980).

Estimation of the damping ratio is problematic, especially for hard-to-sample soils. Some in-situ methods based on cross-hole or down-hole tests have been proposed, but their application is limited by coupling problems in cased boreholes and by difficulties in quantifying geometrical attenuation (Mok *et al.*, 1988). Geophysical non-invasive methods, such as the rise-time method and the spectral ratio method (Jongmans, 1992), give only an approximate estimate of the global quality factor of a soil deposit, with no resolution with depth.

Manuscript received 11 June 2002; revised manuscript accepted 5 February 2003.
Discussion on this paper closes 1 December 2003; for further details see p. ii.
* Department of Structural and Geotechnical Engineering, Politecnico di Torino, Italy; previously Centre for Offshore Foundation Systems, University of Western Australia, Perth.

Surface wave methods are widely used for the determination of the small-strain stiffness of soil deposits. The first applications in geotechnical engineering date back to the end of the 1950s (Jones, 1958), but their popularity began after the introduction of the SASW method (Nazarian & Stokoe, 1984), featuring more rational interpretation and faster in-situ data acquisition. The use of multi-station techniques (Gabriels *et al.*, 1987; Foti, 2000) can lead to even faster and more reliable interpretation processes.

Multi-station measurements can also be used to estimate the spatial attenuation of surface waves, which is closely related to the dissipative behaviour of soils. Seismological studies of surface wave propagation for large-scale events have been used to evaluate the attenuation characteristics of the Earth's crust layers (Anderson *et al.*, 1965) and of large basins (Malagnini *et al.*, 1995). Rix *et al.* (2000) presented a method for estimating the damping ratio from attenuation measurements at small (geotechnical) scale.

More efficient and consistent simultaneous determination and inversion of surface wave dispersion and attenuation characteristics leads to an estimate of both small-strain stiffness and damping ratio of soils (Rix *et al.*, 2001; Lai *et al.*, 2002). In this paper a modified version of the surface wave transfer function method is adopted to characterise the small-strain mechanical behaviour of Pisa Clay.

The paper is divided into three sections. The first section contains a brief geological and geotechnical description of the Leaning Tower of Pisa site. The second section outlines the surface wave transfer function method that has been used for the interpretation of non-invasive seismic tests. Finally the experimental results are presented and compared with previous in-situ and laboratory seismic tests.

THE TESTING SITE

The fame of the Leaning Tower of Pisa is due to foundation settlement, which has caused the tilting of the tower since early on in its construction. Over the last century the

continued tilting created serious concerns about the stability of the tower. Measures for stabilisation have been implemented, and various studies have been carried out at different stages of the stabilisation process. As a consequence, the site is well characterised from a geotechnical point of view.

Several papers and technical reports describe thoroughly the tests performed and their results. Jamiolkowski & Pepe (2001) report some useful references. In this paper only a brief geological description of the soil deposit and the relevant geotechnical properties are reported.

The subsoil consists of three main geological formations, spanning in age from the Holocene to the Pleistocene periods (Costanzo *et al.*, 1995). From the top down, the first formation (A) is predominantly slightly clayey and sandy silt with lenses of sand and clay, and it extends down to a depth of around 10 m (Fig. 1). The underlying clayey formation (B) has a thickness of approximately 30 m, and it can be broadly subdivided into four main layers:

(B1) Upper Clay, also called Pancone Clay
(B2) Intermediate Clay
(B3) Intermediate Sand
(B4) Lower Clay.

The Upper Clay (B1) has a thickness of about 10 m and is a very uniform deposit. Most of the available laboratory test results relate to undisturbed samples retrieved from this layer.

The underlying formation (C) is composed of slightly silty sands and extends to a depth of around 70 m below ground level. A thin and quite stiff slightly cemented layer is reported at approximately 50 m below ground level.

The water table is shallow (2–3 m b.g.l.) and is subject to marked seasonal fluctuations.

An extensive database characterising the mechanical behaviour of the first 30 m b.g.l. can be found in the literature (see Jamiolkowski & Pepe, 2001, for references). In the following discussion only selected results relating to the small-strain behaviour are presented as a framework for the analysis of the results obtained from the surface wave tests.

Jamiolkowski & Pepe (2001) report results of a set of five SCPTs (seismic cone penetration tests), which were carried out in the immediate vicinity of the tower to a depth of 30 m b.g.l. (Fig. 1). The measurements of cone tip resistance indicate the high degree of uniformity of the Pancone Clay and the presence of the sandy layers above and beneath this formation. The measured shear wave velocity shows that, to a depth of about 22 m, the deposit is composed of materials having shear wave velocity < 200 m/s, whereas stiffer materials are found below.

The general trend is confirmed by the results of a cross-hole test performed at the location shown in Fig. 2. As a local direct measurement, the cross-hole gives more accurate results and identifies a slightly stiffer layer inside formation A and the moderately cemented layer in formation C (Fig. 3).

Many high-quality samples from the clayey layers and in particular from the Pancone Clay have been retrieved and tested during previous studies: hence a vast amount of published data is available. Specifically it is worth mentioning the damping ratio measurements reported by Lo Presti *et al.* (1997) on samples retrieved from depths between 12 and 17 m b.g.l. The damping ratio was evaluated during a series of cyclic torsional shear tests identifying values ranging between 2% and 3% in the very small strain range ($\varepsilon_s < 0{\cdot}01\%$). In Fig. 4 the damping ratio at a shear strain of 0·01% is plotted against frequency, showing an almost constant value.

A comparison between the small-strain shear modulus obtained with in-situ (seismic cone) and laboratory (resonant column and bender elements) tests is reported by Jamiolkowski & Pepe (2001).

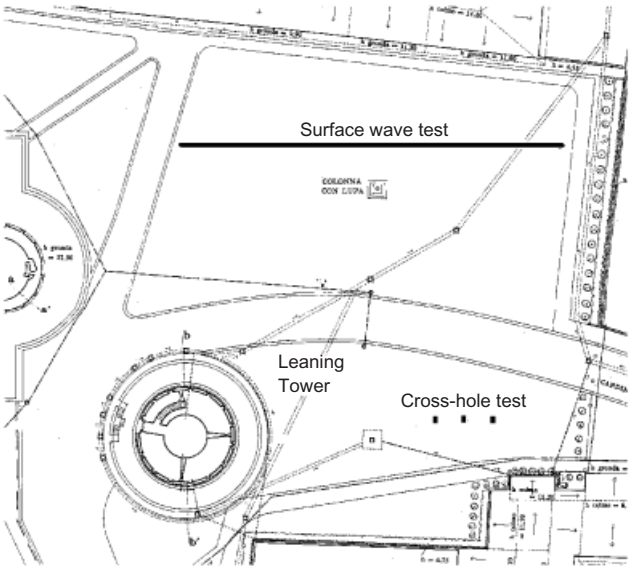

Fig. 2. Cross-hole and surface wave test location

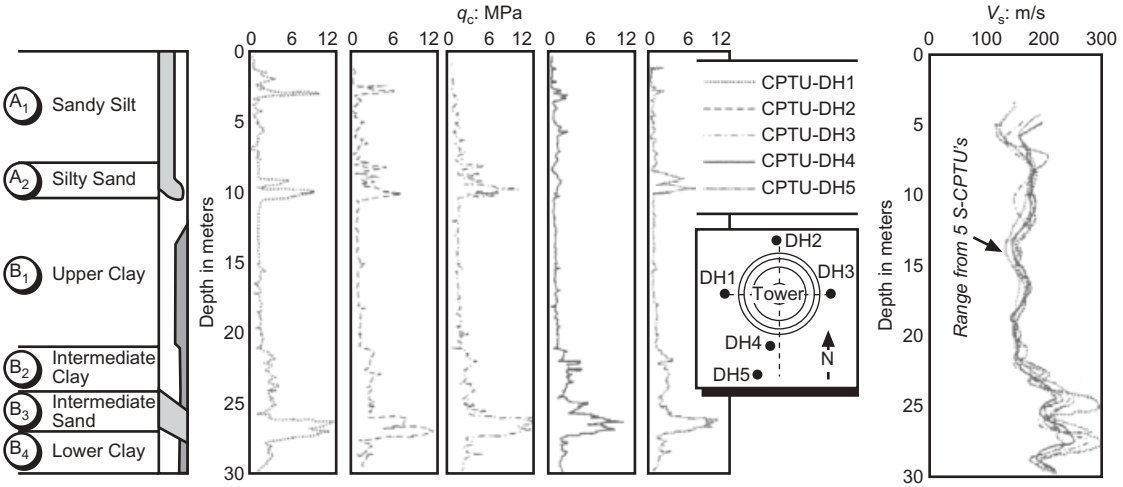

Fig. 1. Schematic stratigraphy and results from seismic cone tests (after Jamiolkowski & Pepe, 2001)

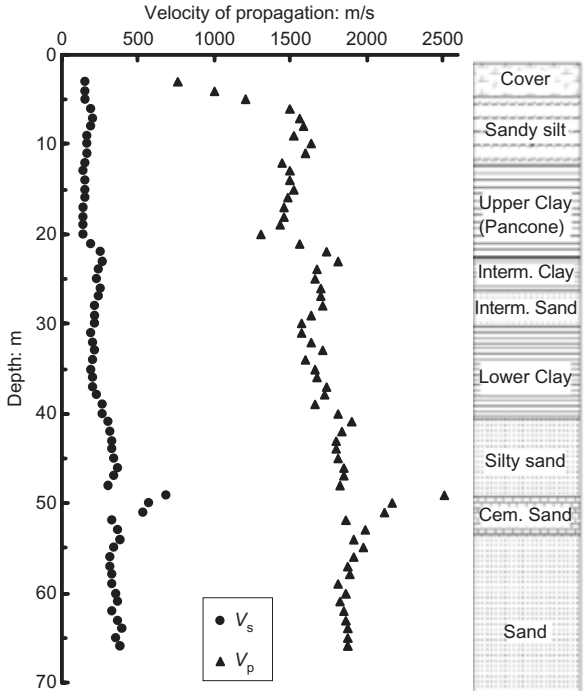

Fig. 3. Borehole log and results from the cross-hole test

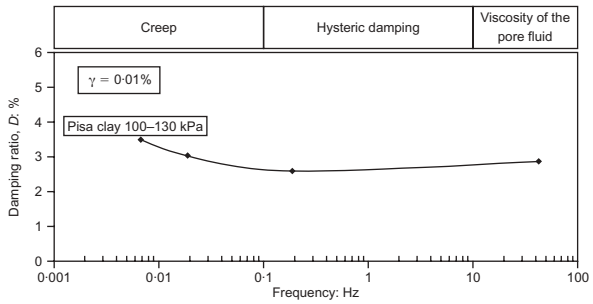

Fig. 4. Shear damping ratio plotted against frequency for Pancone Clay at very small strains (after Lo Presti *et al.*, 1997)

THE SURFACE WAVE TRANSFER FUNCTION METHOD

Rayleigh waves are generated in a solid if a free surface is present. The waves travel along the boundary and are strongly attenuated in the direction perpendicular to the free surface. Plane Rayleigh waves in homogeneous elastic media are non-dispersive and non-dissipative: hence the velocity of their propagation is independent of frequency and their amplitude is not attenuated in space. In vertically heterogeneous media, the velocity of propagation of surface waves is frequency dependent because of geometric dispersion. This phenomenon is the basis for the parameter identification process, in which the relationship between phase velocity and frequency (dispersion curve) is determined from experimental measurements. The experimental dispersion curve is then used in an inversion process to estimate the geometry and small-strain stiffness of the soil deposit, assuming a layered linear elastic model.

The experimental dispersion curve can be estimated from field particle velocity measurements using several techniques (Dziewonski *et al.*, 1969; McMechan & Yedlin, 1981; Nazarian & Stokoe, 1984; Gabriels *et al.*, 1987).

Plane surface waves in a homogeneous elastic medium are not attenuated. Surface waves generated by a point source acting on the ground surface spread along a cylindrical wavefront and hence they suffer a geometrical attenuation that is inversely proportional to the square root of the distance from the source. In dissipative media, material attenuation is added to geometrical attenuation. If material attenuation is experimentally determined, it can be used in an inversion process based on a layered linear viscoelastic model to estimate the small-strain damping ratio. Rix *et al.* (2000) report experimental results obtained using a procedure based on the spatial decay of particle motion along the ground surface.

Experimental dispersion and attenuation curves can be simultaneously determined using a single set of multi-station measurements of particle velocity with the transfer function method introduced by Rix *et al.* (2001). The simultaneous determination is not only effective but also more consistent with a simultaneous inversion of the experimental curves, which is stabler and better posed than two separate inversion processes to determine the stiffness and damping ratio (Lai, 1998). This paper introduces a modified version of the transfer function method, in which the need for the characterisation of the seismic source is eliminated by evaluating the experimental transfer function using a deconvolution process.

The transfer function or frequency response is defined as the ratio between the output and the input of a linear time-invariant system in the frequency domain (Santamarina & Fratta, 1998).

Typically, in a geophysical survey, the ground motion in terms of particle velocities is recorded on the ground surface along a straight line passing through the point of application of the seismic source. Characterisation of the source is a complex task and can be achieved only using controlled sources. Moreover, coupling between the source and the soil is a great concern.

In the proposed procedure the experimental transfer function is evaluated by applying the concept of deconvolution to an ensemble of seismic traces, with no need for the characterisation of the seismic source.

Deconvolution of a signal $f_2(t)$ with a signal $f_1(t)$ is represented in the frequency domain as the ratio between the Fourier transform of the two signals $F_2(\omega)$ and $F_1(\omega)$ respectively:

$$F_{21}(\omega) = \frac{F_2(\omega)}{F_1(\omega)} = \frac{F_2(\omega)\cdot\overline{F_1(\omega)}}{|F_1(\omega)|^2} \tag{1}$$

where ω is the circular frequency.

The spectrum F_{21} contains information about both the interstation phase delay and the attenuation, and represents the dispersion of surface waves between two stations (Dziewonki & Hales, 1972). The phase information is entirely in the numerator on the right side of equation (1), which corresponds to the cross-correlation of the two signal $f_2(t)$ and $f_1(t)$, used in the two-station SASW test for the determination of the phase velocity (Nazarian & Stokoe, 1984).

The deconvolved time signal can be evaluated as

$$\begin{aligned} f_{21}(t) &= \frac{1}{2\pi}\int_{-\infty}^{+\infty}\left[\frac{F_2(\omega)\cdot\overline{F_1(\omega)}}{|F_1(\omega)|^2}\right].\mathrm{e}^{\mathrm{i}\omega t}.\mathrm{d}\,\omega \\ &= \frac{1}{2\pi}\int_{-\infty}^{+\infty}\left[\frac{\mathrm{A}_2(\omega)}{\mathrm{A}_1(\omega)}\right].\mathrm{e}^{\mathrm{i}[\omega t-\phi_2(\omega)+\phi_1(\omega)]}.\mathrm{d}\,\omega \\ &= \frac{1}{2\pi}\int_{-\infty}^{+\infty}\mathrm{A}(\omega).\mathrm{e}^{-i\phi(\omega)}.\mathrm{e}^{\mathrm{i}\omega t}.\mathrm{d}\,\omega \end{aligned} \tag{2}$$

The function f_{21} represents a signal generated by a δ-impulse source acting at the position of the first receiver and detected at the second receiver (Dziewonki & Hales, 1972): therefore F_{21} is equivalent to the transfer function of the system.

Considering a set of multi-station measurements of particle velocity along a straight line on the ground surface, the experimental transfer function $\tilde{F}(r, \omega)$ can be estimated via deconvolution of the whole ensemble of signals:

$$\tilde{F}(r, \omega) = F_{1i}(\omega) = \frac{F_i(\omega)}{F_1(\omega)} \tag{3}$$

where $F_i(\omega)$ is the Fourier Transform of the ith signal detected at distance r from the source, $F_1(\omega)$ is the Fourier transform of the signal detected by the closest receiver, and $F_{1i}(\omega)$ represents the ith deconvolved signal.

The experimental transfer function is then used in a regression process to estimate the dispersion and attenuation curves of surface waves. Modelling the soil as a stack of linear viscoelastic homogeneous layers, it is possible to obtain an analytical expression of the transfer function, which can be used for the regression. For far-field measurements, the vertical displacement $U_z(r, \omega)$ induced by a harmonic source $R_z \cdot e^{i\omega t}$ acting on the ground surface can be expressed as

$$U_z(r, \omega) = R_z \cdot G(r, \omega) \cdot e^{i\left[\omega t - \Psi(r,\omega)\right]} \tag{4}$$

where $\Psi(r, \omega)$ is the complex-valued phase angle and $G(r, \omega)$ is the geometrical spread function (Lai, 1998). Hence, if the response of the receiver placed at $r = r_1$ is used as the reference trace, the transfer function can be written as

$$\tilde{F}(r, \omega) = \frac{U_z(r, \omega)}{U_z(r_1, \omega)} = \frac{G(r, \omega) \cdot e^{-i\Psi(r,\omega)}}{G(r_1, \omega) \cdot e^{-i\Psi(r_1,\omega)}} \tag{5}$$

Assuming $\Psi(r, \omega) = K(\omega) \cdot r$, the implicit dependence of the complex-valued phase angle on the source-to-receiver distance is eliminated, and equation (5) becomes

$$\tilde{F}(r, \omega) = \frac{G(r, \omega)}{G(r_1, \omega)} \cdot e^{-i \cdot K(\omega) \cdot (r - r_1)} \tag{6}$$

where $K(\omega) = \{[\omega / V_R(\omega)] + i\alpha_R(\omega)\}$ is a complex wave number with $V_R(\omega)$ the phase velocity and $\alpha_R(\omega)$ the attenuation coefficient of Rayleigh waves.

The assumption $\Psi(r, \omega) = K(\omega) \cdot r$ is equivalent to considering the phase angle $\Psi(r, \omega)$ to be the result of a single mode of propagation (Rix *et al.*, 2001).

Equation (6) is used in a non-linear regression analysis to estimate the complex-valued wave number $K(\omega)$ from the experimental values of the transfer function.

The experimental complex wave number obtained with the regression procedure contains the information related to both dispersion and attenuation of surface waves and can be used in a complex-valued inversion procedure to estimate both the stiffness and the damping ratio profiles (Rix & Lai, 1998; Lai *et al.*, 2002).

It is worth mentioning that the phase and amplitude of the transfer function could be used for two disjointed regression processes: a linear regression of the phase information leads to an estimate of the dispersion curve, whereas a non-linear regression with an exponential function of the amplitude leads to an estimate of the attenuation.

Linear regression of the phase is basically a multi-station extension of the cross-correlation technique adopted in the two-station SASW test. Indeed, considering only two stations the phase regression gives the same phase difference of the cross-correlation.

The non-linear regression of the amplitude is basically the same procedure as proposed by Rix *et al.* (2000) for the uncoupled determination of Rayleigh wave attenuation.

From a mathematical point of view, coupled regression in complex number space is a more robust procedure than two separate regressions in real number space. Indeed, in the case of a coupled regression, dispersion and attenuation relationships must be simultaneously satisfied by the complex wave number.

EXPERIMENTAL RESULTS

The field measurements were conducted using a 24-channel seismograph and vertical geophones (velocity transducers) having a natural frequency of 4·5 Hz. The typical testing set-up is reported in Fig. 5. Two different seismic impact sources were used to generate energy over a broad frequency range: a large weight-drop system (130 kg released under self-weight from a height of 3 m above the ground surface) and a sledgehammer for long and short arrays respectively. The need for two different testing configurations is due to the trade-off between the length of the array and the frequency band.

The test location is shown in Fig. 2. The length of the survey prevented the execution of the surface wave test in the same location of the cross-hole survey. Nevertheless, the relatively homogeneous conditions across the site allow a comparison of the results to be made.

As equal receivers are used at each location, their frequency response is considered equivalent, and the experimental transfer function is evaluated directly from equation (3).

In the analysis the geometric spreading function $G(r, \omega)$ has been assumed to be proportional to $1/\sqrt{r}$: hence equation (6) simplifies to

$$\tilde{F}(r, \omega) = \frac{\sqrt{r_1}}{\sqrt{r}} \cdot e^{-i \cdot K(\omega) \cdot (r - r_1)}. \tag{7}$$

The complex wave number, $K(\omega)$, is obtained by minimising the L_2-norm of the difference between the experimental and the predicted transfer functions

$$\sum_N \left\{ \left[\tilde{F}_{exp}(r, \omega) - \frac{\sqrt{r_1}}{\sqrt{r}} \cdot e^{-i \cdot K(\omega) \cdot (r - r_1)} \right] \cdot \text{conj} \left[\tilde{F}_{exp}(r, \omega) - \frac{\sqrt{r_1}}{\sqrt{r}} \cdot e^{-i \cdot K(\omega) \cdot (r - r_1)} \right] \right\} = \min \tag{8}$$

where N is the total number of sensors and conj[...] denotes the complex conjugate.

In order to assess the importance of near-field effects and non-linearities, the regression process is repeated, discarding the reading at the closest receivers, and the regression with the minimum misfit is selected.

Comparison between the experimental data and the regression analysis is reported in Fig. 6 for a frequency of

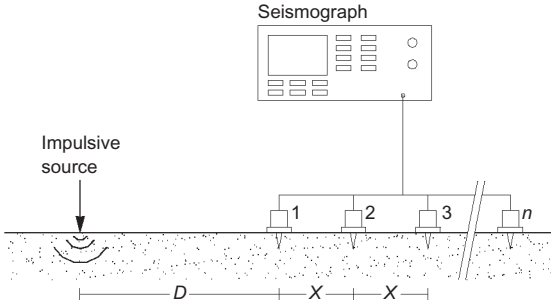

Fig. 5. Multi-station testing set-up

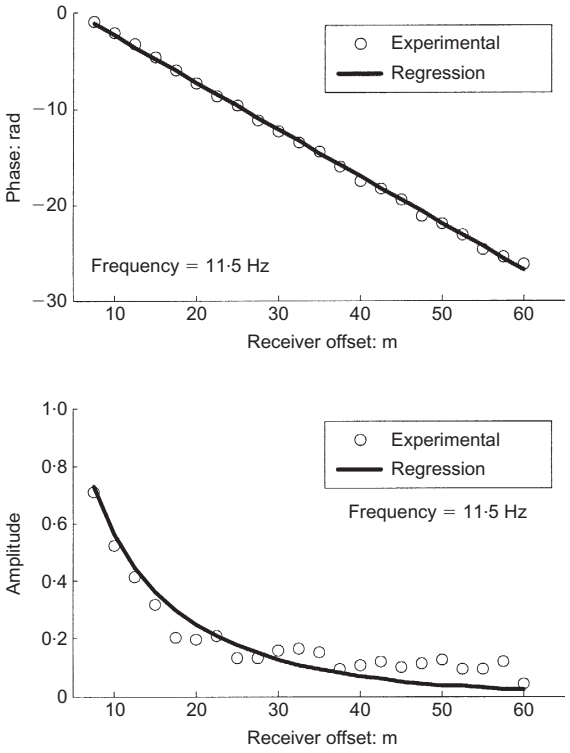

Fig. 6. Comparison between experimental transfer function and model

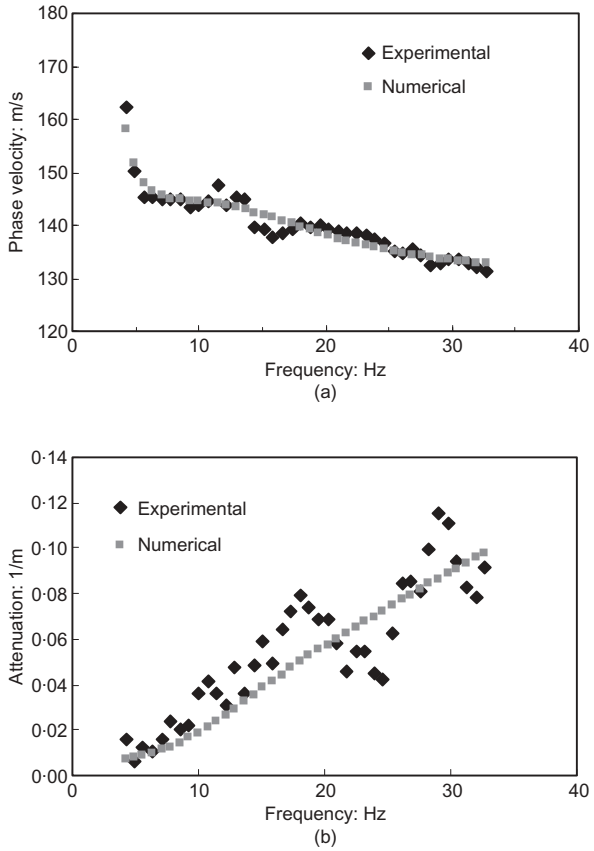

Fig. 7. (a) Dispersion and (b) attenuation curves of surface waves

11·5 Hz. The results are shown in terms of phase and amplitude of the transfer function rather than in terms of real and imaginary components. Indeed, phase and amplitude have a clear physical meaning, as they are linked to phase velocity and attenuation of surface waves respectively. A satisfactory fit between the experimental data and the model has been obtained.

The regression process is repeated over the entire frequency range of interest to estimate the variation of the complex wave number with frequency. Although the experimental complex wave number could be directly used for an inversion process for the evaluation of the parameters of the layered linear viscoelastic model, experimental dispersion and attenuation curves (Fig. 7) are the usual input of inversion codes. The inversion process has been carried out using the code SURF developed by Robert Herrmann at St Louis University (Herrmann, 1994). Solving the inverse problem by using a weighted and damped least-square algorithm, the code leads to an estimate of soil parameters (shear wave velocity and damping ratio) and layer thicknesses for a stack of homogeneous layers. The values of the numerical dispersion and attenuation curves obtained at the last iteration of the inversion process are in good agreement with the experimental values (Fig. 7).

In the inversion process it is assumed that the strain level does not affect the experimental dispersion and attenuation curves. This assumption is well in agreement with the commonly accepted idea that strain levels induced during geophysical seismic tests are very small in the far field. Indeed, the energy associated with the sources and the distance at which the receivers are placed (not less than 1 m for the sledgehammer and not less than 3 m for the weight drop system) are such that the strain level is always very small.

The shear wave velocity and damping ratio profiles obtained from the surface wave analysis are shown in Fig. 8 and compared respectively with the data from the in-situ cross-hole test and with a reference value from laboratory testing. The latter has been estimated in the frequency range covered by surface wave data (5–40 Hz). In this frequency range an almost constant value of the damping ratio has been obtained in laboratory tests (Fig. 4).

A step-by-step summary of the entire procedure adopted for the analysis of the experimental surface wave data is reported in Table 1, with reference to the relevant equations and figures.

The shear wave velocity, V_S, can be used to estimate the small-strain shear modulus, G_0, using the elastic relationship $G_0 = \rho V_S^2$, (where ρ is the soil density). Fig. 9 reports a comparison between several estimates of the small-strain stiffness at the Pisa site from both in-situ and laboratory tests.

CONCLUSIONS

Surface wave data are usually inverted to get an estimate of the small-strain shear modulus profile. The innovative transfer function approach adopted in this work has led to a reliable estimate of both the small-strain shear modulus and the damping ratio, in good agreement with the results of other in-situ and laboratory tests. It is worth recalling that surface wave methods are based on indirect measurements: hence they give average values of the mechanical parameters over large volumes of soils, whereas other tests generate more accurate (and more expensive) local estimates. The potential depth of investigation of surface wave tests is influenced by the available space for testing along the ground surface and by the amount of energy released by the seismic source.

The surface wave transfer function method can be considered a valuable option to obtain the damping ratio of soils,

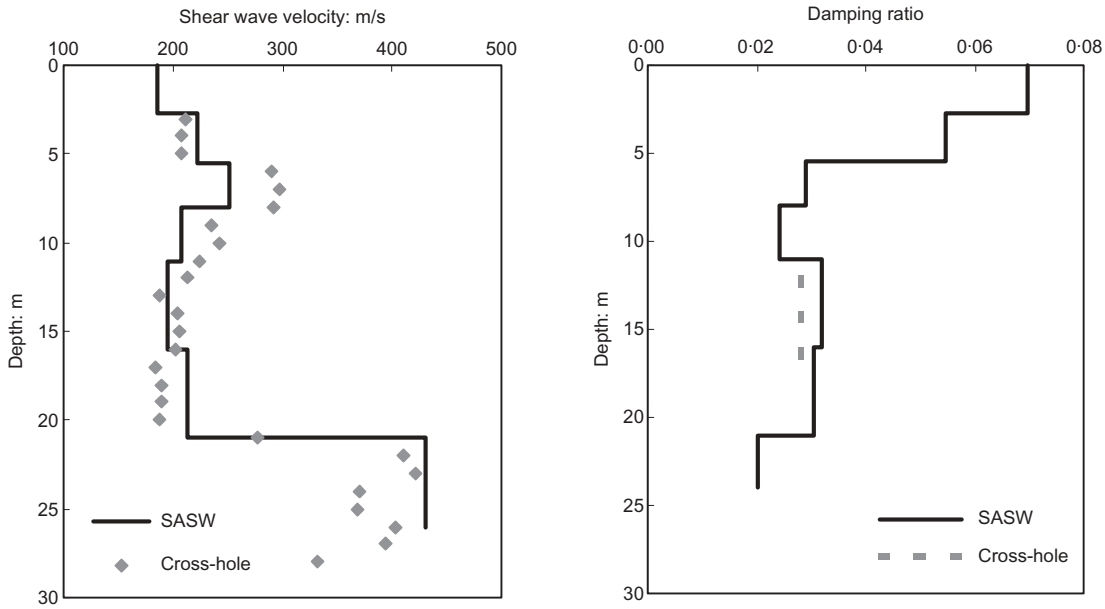

Fig. 8. Shear wave velocity and damping ratio profile from surface wave test

Table 1. From field data to shear wave velocity and damping ratio profiles: step-by-step procedure

Step 1	Field measurements: time histories of particle velocities $f_i(t)$ $i = 1, 2, \ldots, N_{\text{receivers}}$	Fig. 5
Step 2	Particle velocity spectra: $F_i(\omega) = \text{FFT}[f_i(t)]$ $i = 1, 2, \ldots, N_{\text{receivers}}$	
Step 3	Experimental transfer function: $\tilde{F}_{\text{exp}}(r, \omega) = \dfrac{F_i(\omega)}{F_1(\omega)}$	Equation (3)
Step 4	Regression process: $L_2[\tilde{F}_{\text{exp}}(r, \omega) - \tilde{F}_{\text{analytical}}(r, \omega)] = \min \rightarrow K(\omega)$	Equation (8); Fig. 6
Step 5	Dispersion: $V_{\text{R}}(\omega) = \dfrac{\omega}{\text{real}[\text{K}(\omega)]}$ Attenuation: $\alpha_{\text{R}}(\omega) = \text{imag}[\text{K}(\omega)]$	Fig. 7
Step 6	Rayleigh wave inversion process: $V_{\text{R}}(\omega)$ and $\alpha_{\text{R}}(\omega) \rightarrow V_{\text{S}}(z)$ and $D_{\text{S}}(z)$	Fig. 8

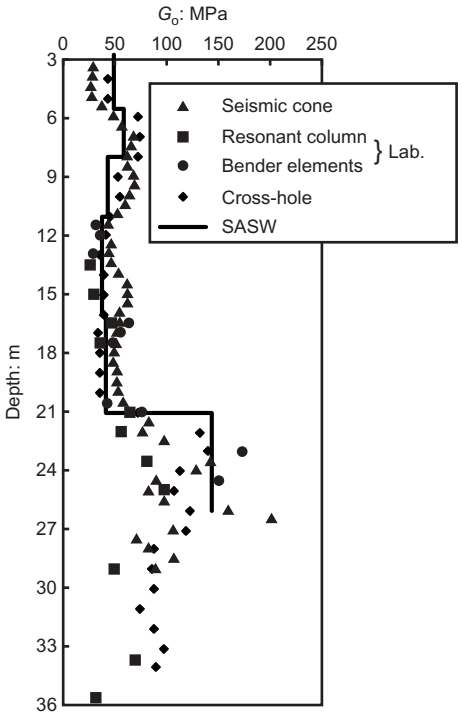

Fig. 9. Small-strain shear modulus from in-situ and laboratory tests (modified after Jamiolkowski & Pepe, 2001)

which typically is complex to estimate, especially for hard-to-sample soils. However, it should be considered that a slight overestimation of the dissipative properties of the medium is to be expected, as attenuation mechanisms other than geometrical spreading can interfere with the intrinsic attenuation.

The proposed procedure leads to the estimation of the experimental transfer function with no need for the use of special seismic sources. Moreover, it does not require any particular testing geometry: hence it can be used for the analysis of conventional multi-station seismic data.

ACKNOWLEDGEMENTS

The author is grateful to Mr R. Maniscalco and Dr L. V. Socco for help in the acquisition of the field data, and to Professor R. Lancellotta for his valuable insights into the topic. Dr S. Gourvenec kindly reviewed and improved the manuscript. Invaluable suggestions by Professor C. Santamarina are also gratefully acknowledged.

This work has been supported by the Italian Ministry for University and Scientific Research, under grant MURST 40% 1998, 'Geotechnical Analysis for Seismic Vulnerability of Historical Buildings'.

NOTATION

$A(\omega)$	amplitude of Fourier transform $F(\omega)$
conj[...]	complex conjugate operator
D	damping ratio
$f(t)$	seismic signal
$F(\omega)$	Fourier transform of the signal $f_i(t)$
$f_{21}(t)$	deconvolution in time domain
$F_{21}(\omega)$	deconvolution in frequency domain (defined by equation (1))
$\tilde{F}_{\text{exp}}(r, \omega)$	experimental transfer function
G_0	small-strain shear modulus
$G(r, \omega)$	geometrical spread function
i	imaginary unit
$K(\omega)$	complex wave number
Q	quality factor
r	source-to-receiver distance
R_z	harmonic source magnitude
t	time
$U_z(r, \omega)$	vertical displacement induced by surface waves generated by a harmonic source
V_R	Rayleigh wave phase velocity
V_S	shear wave velocity (S-wave)
α_R	Rayleigh wave attenuation coefficient
ρ	mass density
$\phi(\omega)$	phase of the Fourier transform $F(\omega)$
$\Psi(r, \omega)$	phase angle of $U_z(r, \omega)$
ω	circular frequency

REFERENCES

Aki, K. & Richards, P. G. (1980). *Quantitative seismology: theory and methods*. San Francisco: Freeman.

Anderson, D. L., Ben-Menahem, A. & Archambeau, C. B. (1965). Attenuation of seismic energy in the upper mantle. *J. Geophys. Res.* **70**, 1441–1448.

Costanzo, D., Jamiolkowski, M., Lancellotta, R. & Pepe, M. C. (1995). Leaning Tower of Pisa: description of the behaviour. *Proc. 11th African Regional Conf. Soil Mech. and Found. Engng, Cairo*, **1**, 1–55.

Dziewonski, A., Bloch, S. & Landisman, M. (1969). A technique for the analysis of transient seismic signals. *Bull. Seismol. Soc. Am.* **59**, 427–444.

Dziewonki, A. M. & Hales, A. L. (1972). Numerical analysis of dispersed seismic waves. In *Methods in computational physics*, vol.11, *Seismology: Surface waves and earth oscillations* (ed. B. A. Bolt), pp. 39–85. New York: Academic Press.

Foti, S. (2000). *Multi-station methods for geotechnical characterisation using surface waves*. PhD dissertation, Politecnico di Torino, Italy.

Gabriels, P., Snieder, R. & Nolet, G. (1987). In situ measurements of shear-wave velocity in sediments with higher-mode Rayleigh waves. *Geophys. Prospect.* **35**, 187–196.

Herrmann, R. B. (1994). *Computer programs in seismology: SURF*, User's Manual. Missouri: St Louis University.

Ishihara, K. (1996). *Soil behaviour in earthquake geotechnics*. Oxford: Oxford University Press.

Jamiolkowski, M. & Pepe, M. C. (2001). Vertical yield stress of Pisa clay from piezocone tests. *J. Geotech. Geoenviron. Engng, ASCE* **127**, 893–897.

Jongmans, D. (1992). The application of seismic methods for dynamic characterisation of soils in earthquake engineering. *Bull. Int. Assoc. Engng Geol.* **46**, 64–69.

Jones, R. B. (1958). In-situ measurement of the dynamic properties of soil by vibration methods. *Géotechnique* **8**, No. 1, 1–21.

Kramer, S. L. (1996). *Geotechnical earthquake engineering*. New York: Prentice Hall.

Lai, C. G. (1998). *Simultaneous inversion of Rayleigh phase velocity and attenuation for near-surface site characterization.* PhD dissertation, Georgia Institute of Technology, Atlanta.

Lai, C. G., Rix, G. J., Foti, S. & Roma, V. (2002). Simultaneous measurement and inversion of surface wave dispersion and attenuation curves. *Soil Dynam. Earthquake Engng*, **22**, No. 9–12, pp. 923–930.

Lo Presti, D. C. F., Pallara, O. & Cavallaro, A. (1997). Damping ratio of soils from laboratory and in-situ tests. *Proc. 14th Int. Conf. Soil Mech. Found. Engng*, 391–400, Balkema: Rotterdam.

Malagnini, L., Herrmann, R. B., Biella, G. & de Frando, R. (1995). Rayleigh waves in quaternary alluvium from explosive sources: determination of shear-wave velocity and Q structure. *Bull. Seismol. Soc. Am.* **85**, 900–922.

McMechan, G. A. & Yedlin, M. J. (1981). Analysis of dispersive waves by wave field transformation. *Geophysics* **46**, 869–874.

Mok, Y. J., Sanchez-Salinero, I., Stokoe, K. H. II & Roesset, J. M. (1988). In situ damping measurements by crosshole seismic method. *In Earthquake engineering and soil dynamics II: Recent advances in ground motion evaluation*, ASCE Geotechnical Special Publication No. 20 (ed. J. L. Von Thun), pp. 305–320. American Society of Civil Engineers, New York.

Nazarian, S. & Stokoe, K. H. II (1984). In situ shear wave velocities from spectral analysis of surface waves. *Proc. 8th Conf. Earthquake Engng, San Francisco* **3**, 31–38.

Rix, G. J. & Lai, C. G. (1998). Simultaneous inversion of surface wave velocity and attenuation. In *Geotechnical site characterization* (eds P. K. Robertson and P. W. Mayne), pp. 503–508. Rotterdam: Balkema.

Rix, G. J., Lai, C. G. & Spang, A. W. (2000). In situ measurements of damping ratio using surface waves. *J. Geotech. Geoenviron. Engng, ASCE* **126**, No. 5, 472–480.

Rix, G. J., Lai, C. G. & Foti, S. (2001). Simultaneous measurement of surface wave dispersion and attenuation curves. *Geotech. Test. J., ASTM* **24**, No. 4, 350–358.

Santamarina, J. C. & Fratta, D. (1998). *Discrete signals and inverse problems in civil engineering*. New York: ASCE Press.